# Importance of Multiple-Scattering Phenomena in XAS Structural Determinations of $[Ni(CN)_4]^{2-}$ in Condensed Phases

**Adela Muñoz-Páez,*,† Sofía Díaz-Moreno,‡ Enrique Sánchez Marcos,§ and John J. Rehr||**

Instituto de Ciencia de Materiales and Departamento de Química Inorgánica, CSIC-Universidad de Sevilla, c/Américo Vespucio s/n, 41092 Sevilla, Spain, European Synchrotron Radiation Facility (ESRF), 6 Jules Horowitz, Grenoble Cedex 9, France, Departamento de Química Física, Universidad de Sevilla, 41012 Sevilla, Spain, and Department of Physics, University of Washington, Seattle, Washington 98195-1560

*Received March 10, 2000*

A quantitative analysis of the XAS spectra of the tetracyanonickelate complex $[Ni(CN)_4]^{2-}$ has been carried out. The simultaneous study of the EXAFS and XANES regions yielded complementary information regarding the geometric and electronic structures of the complex. XANES spectra were modeled by applying recently developed self-consistent, full multiple-scattering algorithms in the FEFF8 code (version 8x34). XANES spectra for clusters of different sizes (from 9 to 125 atoms) were computed and compared with experimental spectra. This region of the spectra was proportional to a broadened Ni p-density of states diagram above the Fermi level. Although the main features of the XANES spectra were reasonably reproduced by computations, the weak dependence of the theoretical spectra on cluster size contrasts with the close similarity between the experimental spectra of the solid and solution systems. Because of the special geometry of the complex, calculations with polarized light parallel and perpendicular to the molecular plane were carried out, yielding a reasonable reproduction of the experimental data from another report for cluster sizes equal to or higher than 45 atoms. The highly symmetric square planar structure of the complex was found to be responsible for the unusual amplitude of the multiple-scattering (MS) contributions to the EXAFS spectra. Spectra in this region were fitted using the FEFFIT EXAFS analysis program, taking into account only the MS paths that simultaneously have both a high amplitude, as calculated with the ab initio code FEFF, and a small Debye−Waller factor, as estimated by the *independent-vibration approximation* model. Fitting results yielded very similar structures for the $Ni^{2+}$ complex in the solid state and in solution, though the larger Debye−Waller factors found for the solid suggest higher static disorder in this state.

## Introduction

Tetracyanonickelate(II) is one of the most stable $Ni^{2+}$ complexes, with a high overall formation constant ($\log \beta_4 \approx 30.5$). It presents a square planar structure, being stable both in aqueous solutions and in the solid state.[1] The interest in square planar complexes of transition metals, particularly those of group 10, stems in part from their unusual electronic spectra and electrical properties. For instance, mixed-valence $Pt(CN)_4^{x-}$ complexes are the most representative one-dimensional electrical conductors.[2] The bonding structure of mononuclear cyanide complexes is similar to that of analogous carbonyl complexes, and can be described in terms of ligand to metal charge donation through $\sigma$ bonds and metal to ligand $\pi$ back-bonding.[3] Nevertheless, such a qualitative molecular picture cannot explain the singular electrical properties of the polynuclear complexes; instead detailed electronic structure calculations are required.

Concerning the geometry of these systems, the crystal structures have been determined for potassium, cesium, barium, sodium, strontium, and pyridinium anhydrous and partially hydrated salts.[4] Although the electronic spectra point to the existence of a symmetric complex in aqueous solution,[5] heretofore there has been no direct information concerning the structure of the dissolved species. Moreover, the geometric structure seems to be strongly affected by the degree of hydration, so that a given complex might show different structures depending upon the number of crystallization water molecules. For this reason, it would be of interest to obtain structural information from these type of systems with various degrees of hydration. The existence of rigid structures with strong M−C and C−N bonds makes them good candidates to be studied by X-ray absorption spectroscopies, which could provide both the electronic and geometric structures of the anhydrous solid-state salts and of the dissolved species.

The X-ray absorption spectrum of the powdered potassium salt was first obtained more than 20 years ago,[6] but the resolution

* Corresponding author. E-mail: adela@cica.es. Fax: 34-95-4460665.
† Departamento de Química Inorgánica, Universidad de Sevilla.
‡ ESRF.
§ Departamento de Química Física, Universidad de Sevilla.
|| University of Washington.

(1) *Comprehensive Coordination Chemistry*; Wilkinson, G., Gillard, R. D., McCleverty, J., Eds.; Pergamon: New York, 1987; Vols. 2 and 5.
(2) Muller, S. *Structural Inorganic Chemistry*; Wiley: London, 1992.
(3) Miessler, G. L.; Tarr, D. A. *Inorganic Chemistry*; Prentice Hall: Engelwood Cliffs, NJ, 1991; p 290.
(4) (a) Vannerberg, N. G. *Acta Chem. Scand*. **1964**, *18*, 2385. (b) Larsen, F. K.; Hazell, R. G.; Rasmussen, S. E. *Acta Chem. Scand.* **1969**, *23*, 61. (c) Musselman, R. L.; Stecher, L. C.; Watkins, S. F. *Inorg. Chem.* **1980**, *19*, 3400. (d) Leipoldt, J. G.; Basson, S. S.; Bok, L. D. C. *Acta Crystallogr*. **1970**, *B26*, 361. (e) Leipoldt, J. G.; Basson, S. S.; Bok, L. D. C. *Acta Crystallogr*. **1969**, *B25*, 579.
(5) Cowman, C. D.; Ballhausen, C. J.; Gray, H. B. *J. Am. Chem. Soc*. **1973**, *95*, 7873.
(6) Umadikar, P. H.; Mestry, S. G.; Bath, N. V.; Hadler, B. C. *Spectrochim. Acta* **1976**, *31B*, 411.
(7) Kosugi, N.; Yokoyama, T.; Kuroda, H. *Chem. Phys*. **1986**, *104*, 449.

10.1021/ic000274n CCC: $19.00 
Published on Web 07/21/2000

of this spectrum was very poor because it was not recorded at a synchrotron source. Further measurements of the XANES region,[7−9] at the Photon Factory (KEK, Tsukuba, Japan), with polarized light yielded better resolution, revealing a peculiar shape with an intense preedge peak, not usual for centrosymmetric systems. Concerning the EXAFS region, these highly symmetric and very stable complexes with two-atom ligands each show an amplitude of the second peak in the Fourier transform (FT) as high as that of the first peak, as observed for systems containing this complex[10] or the mercury[11] and iron[12] cyanides $[Hg(CN)_2]$, $[Fe(CN)_6]^{3-}$, and $[Fe(CN)_6].^{4-}$ Similarly, for the EXAFS spectra of molybdenum,[13] $[Mo(CO)_6]$, iron,[14] $Na_2[Fe(CO)_4]$, and rhodium,[15] $[Rh(CO)_2Cl_2]$, carbonyls, the amplitude of the second peak in each FT is even higher than that of the first.

The peculiar features in the edge region and the extremely high amplitude of the second peak of the FT of each EXAFS spectrum point to the need for using a multiple-scattering (MS) approach in a quantitative analysis of the XAS spectra of $[Ni(CN)_4]^{2-}$ units. Although they are among the best examples to show the relevance of multiple-scattering contributions, for only two of the above-mentioned systems were attempts made to take MS contributions into account.[10,14] Recently, several approaches were made to this problem, and several packages are now available that take into account MS contributions in the analysis of the EXAFS functions.[16−18] This type of approach is not used as often as desired, probably because it requires additional strategies to reduce the high number of free parameters appearing with the inclusion of a large number of paths.

Herewith we present a refined quantitative analysis of the XANES and EXAFS spectra of the tetracyanonickelate(II) complex, which yield complementary information. Although MS contributions were taken into account to fit the EXAFS region, only four paths were considered in the analysis of this region, which yielded detailed information about the geometry of the complex both in the solid state and in solution. The study of the XANES region yielded information about the electronic structure of this system, i.e., the Fermi level energy and a density of states diagram. The simultaneous quantitative analysis of the two regions allowed a comparison of the structural information provided by both. For instance, it provided an answer to the question of whether both regions show the same sensitivity to long range order or to static disorder.

## Methods

**Experimental Details.** $K_2[Ni(CN)_4]$ was obtained from Sigma-Aldrich. This compound is very sensitive to humidity, undergoing changes in the number of crystallization water molecules and, concomitantly, some physical properties such as color after exposure to moisture. For this reason, two spectra of the solid compound were recorded, the first one for a sample as received and the other for a sample after being dried overnight at 110 °C. No differences were observed between the spectra.

The X-ray absorption spectra of the Ni K edge (8333 eV) of the $K_2[Ni(CN)_4]$ complex in the solid state and in a 0.1 *m* aqueous solution were recorded at Station BL 10B of the Photon Factory National Laboratory for High Energy Physics, KEK. All measurements were carried out at room temperature in the transmission mode using a high-resolution Si(311) channel cut monochromator. A 17 cm long ion chamber filled with $N_2(g)$ was used to monitor the incoming beam, and a 31 cm long ion chamber filled with a 75% $N_2(g)$−25% Ar(g) mixture was used to monitor the transmitted beam. Energy calibration was carried out with a copper foil. For the K-edge spectrum of this metal, the first inflection point was reported to appear at 8979 eV and the small, well-resolved peak at the edge, which is used as a reference, to appear 2.3 eV above. The ring energy was 2.5 GeV and the ring current 300 mA. Each data point was collected for 1 s, and several scans were averaged to improve statistical quality. To measure the solid compound, the appropriate amount of complex to bring the total absorbance to $\mu x = 2.5$ was mounted onto a self-supporting sample holder. The aqueous solution was measured in a variable path length cell,[19] which was necessary for optimization of the absorption edge jump, being the depth of the liquid vein, 3.5 mm.

**Computations.** Full multiple-scattering (FMS) calculations were carried out to reproduce the XANES region using self-consistent muffin-tin potentials and the real-space multiple-scattering (RSMS) formalism of the FEFF8 code, as described in ref 18. This procedure is based on Green's function multiple-scattering calculations in the complex energy plane, rather than on the use of wave functions or molecular orbitals. The self-consistent-field (SCF) procedure yields an ab initio calculation of the electronic structure, including the threshold of Fermi energy and the electron energy distribution (i.e., the angular momentum projected local density of states or LDOS) in the cluster. This approach thereby increases the first-principles character of XAS calculations and their interpretation as it permits simultaneous calculations of both LDOS and XANES, as well as charge-transfer and other chemical effects in XANES. The calculations here were carried out with the experimental version x34 of FEFF8, which is essentially equivalent to the release version. Several energy-dependent exchange correlation potentials were tested, and the default Hedin−Lundqvist model appeared to be the best for the system here studied. The FEFF8 code gains efficiency by permitting FMS calculations within a small sphere of radius "rfms" and uses a high-order MS path expansion outside that sphere. To make possible the reproduction of the XANES calculations, a sample FEFF input file is included as Supporting Information in Table 1S.

To isolate the EXAFS wave, standard procedures were used to perform background removal.[20] Normalization was carried out by division by the edge step. In a first approach, the edge energy was chosen as the maximum in the first derivative in the main rise of the absorption spectrum. To analyze the EXAFS spectra of the complex in the solid state and in aqueous solutions, a path analysis was used (rfms = 0). As a first step, a calculation of the contribution to the EXAFS signal of each important scattering path, either single- or multiple-scattering (SS or MS) paths, was performed with FEFF8x34. Initially the mean square displacements $\sigma^2$ were set to zero for all paths, and the amplitude reduction factor $S_o^2$ was set equal to 1. Also, the default plane wave amplitude filter equal to 2.5% and a curved wave amplitude filter equal to 4.0% of the amplitude of the first single scattering path were used, as in FEFF7. The EXAFS signals calculated for the MS paths thus obtained were used to fit the experimental spectra by employing the XAFS analysis program FEFFIT.[21] To minimize the number of free parameters used during the fitting procedure, an "independent vibration approximation" model[22] was used to define the values of $\sigma^2$ for the MS paths as a function of those from SS paths.

(8) Kosugui, N. In *X-ray Absorption Fine Structure for Catalysts and Surfaces*; Iwasawa Y., Ed.; Springer-Verlag: Berlin, 1996; p 60.
(9) Hatsui, T.; Takata, Y.; Kosugi, N. *J. Synchrotron Rad.* **1999**, *6*, 376.
(10) Jones, M. J.; Harris, K. D. M.; Sankar, G.; Maschmeyer, T.; Thomas, J. M. *J. Chem. Soc., Faraday Trans.* **1996**, *92*, 1046.
(11) Akesson, R.; Persson, I.; Sandström, M.; Wahlgrem, U. *Inorg. Chem.* **1994**, *33*, 3715.
(12) Bianconi, A.; Dell'Ariccia, M.; Durham, P. J.; Pendry, J. B. *Phys. Rev. B* **1982**, *26*, 6502.
(13) Cramer, S. P.; Hodgson, K. O.; Stiefel, E. I.; Newton, W. E. *J. Am. Chem. Soc*. **1978**, *100*, 2748.
(14) Teo, B. K. *J. Am. Chem. Soc*. **1981**, *103*, 3990.
(15) Van't Blik, H. F. J.; van Zon, J. B. A. D.; Huizinga, T.; Vis, J. C.; Koningsberger, D. C.; Prins, R. *J. Am. Chem. Soc*. **1985**, *107*, 3139.
(16) Gurman, S. J.; Bisntead, N.; Ross, I. *J. Phys. C* **1984**, *17*, 143.
(17) Filipponi, A.; Di Cicco, A.; Natoli, C. R. *Phys. Rev. B* **1995**, *52*, 15122.
(18) Ankudinov, A. L.; Ravel, B.; Rehr, J. J.; Conradson, S. D. *Phys. Rev. B* **1998**, *58*, 7565.
(19) Sánchez Marcos, E.; Gil, M.; Martínez, J. M.; Muñoz-Páez, A.; Sánchez Marcos, A. *Rev. Sci. Instrum.* **1994**, *65*, 2153.
(20) Cook, J. W.; Sayers, D. E. *J. Appl. Phys.* **1981**, *52*, 5024.
(21) Stern, E. A.; Newville, M.; Ravel, B.; Yacoby, Y.; Haskel, D. *Physica B* **1995**, *208−209*, 117.

This model has been applied successfully to other systems.[23,24] Sample FEFF and FEEFIT input and output files similar to those used in the EXAFS analysis are included as Supporting Information in Tables IIS−IVS.

## Results and Discussion

**XANES Spectra.** Figure 1a shows the XANES region of the X-ray absorption spectra of $K_2[Ni(CN)_4]$ in the solid state and in aqueous solution. Both spectra are quite similar, but some slight differences between them can be observed. The main difference is the clear shoulder in the edge step for the solid compound, which for the dissolved system broadens to a change in slope. Moreover, the main peak after the edge is sharper for the solid system. The close similarity between solid and solution systems, already observed in mercury[11] and thallium[25] cyano complexes, $[Hg(CN)_2]$ and $[Tl(CN)_4]^-$, and in yttrium thiocyanate[26] complexes, points to the fact that the multiple-scattering resonances that contribute most significantly to this region of the spectrum are mainly due to atoms within the well-defined molecular complex, which in this case is formed by 9 atoms. Nevertheless there should be nonnegligible effects due to factors in the environment of this complex: (a) electronic factors and (b) scattering factors as well as disorder. The first set of factors account for changes induced in the electron distribution of the basic units by the interactions with the environment of the condensed phase. The second take into account the increased number of scattering paths appearing in larger clusters, together with the damping effects of disorder.

To investigate cluster size effects on XANES spectra, several calculations were performed with an increasing number of atoms using the atomic coordinates of the crystalline anhydrous system. The values reported from XRD measurements for Ni−C distances are 1.84 and 1.90 Å, while the corresponding Ni−N bond distances are 2.95 and 3.04 Å.[4a] These calculations start with the basic 9-atom ensemble of $[Ni(CN)_4]^{2-}$ and then increase the number of additional shells up to 125 atoms. Figure 1b shows the calculated XANES spectra for the various clusters after the Fermi level is shifted down 1 eV (to correct the slightly high FEFF8 estimate) and a reduction in the line broadening of 0.1 eV is applied. (A typical input file for these calculations appears in Table IS.) Remarkably, even the smallest 9-atom cluster roughly reproduces the main features of the spectrum. Although there is an improvement for larger cluster sizes, some of the features, such as the intensity of the sharp preedge peak, are not adequately reproduced even for the 125-atom cluster. Moreover, the variations of the spectra with cluster size show that the preedge region does not converge monotonically with size; however the features do systematically sharpen with increasing size. Additionally, the appearance of a clear shoulder in the main rise and a decrease in the intensity of the broad resonance at about 8370 eV are observed as the cluster size increases. The spectra calculated for cluster sizes equal to or larger than 78 atoms do not show significant changes, and thus LDOS and polarization-dependent calculations were made for clusters up to this size.

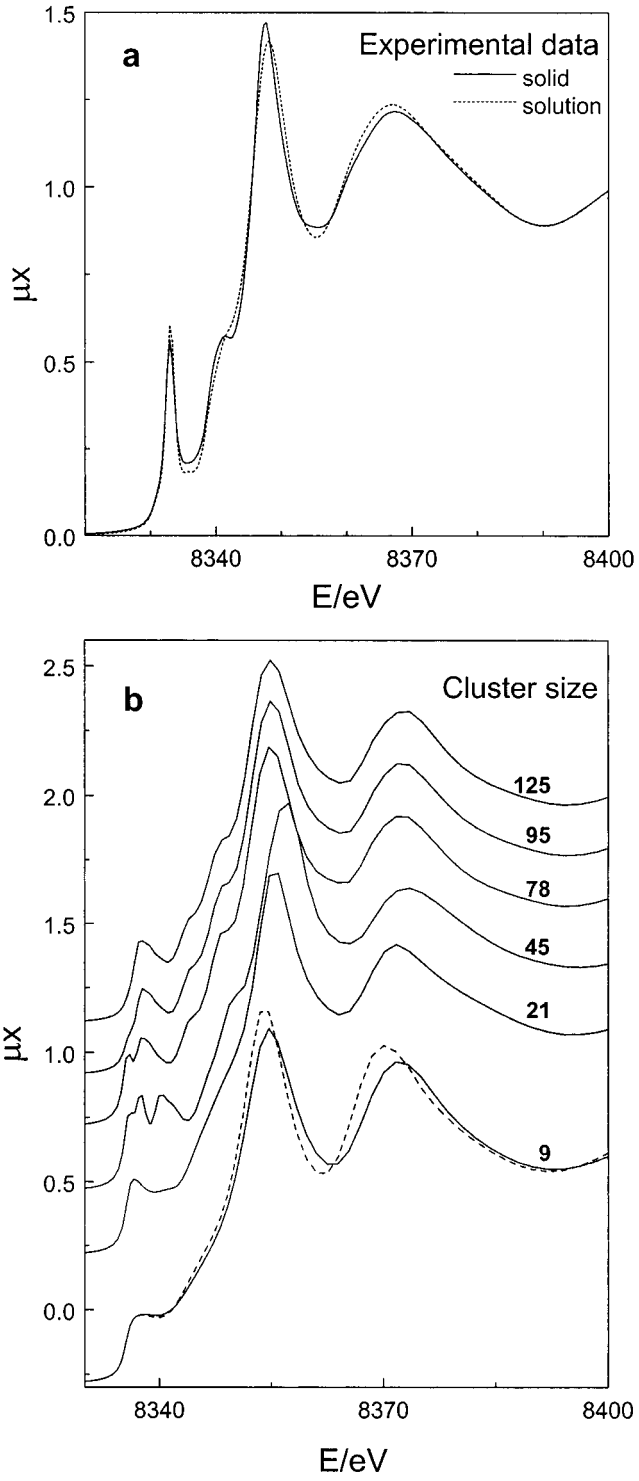


**Figure 1.** (a) XANES region of the Ni K-edge X-ray absorption spectra of $K_2[Ni(CN)_4]$ in the solid state and in a 0.1 *m* aqueous solution. (b) Full multiple-scattering calculation of the XANES spectra for a system with the atomic coordinates of crystalline $K_2[Ni(CN)_4]$, for clusters with increasing numbers of atoms: 9, 21, 45, 78, 95, and 125 (solid lines). The dashed line shows similar calculation for the 9-atom symmetric cluster.

It should be noted that the so-called preedge peak and the shoulder in the step are more sensitive to the "small-cluster" size considered in the full multiple-scattering computations (defined by the cluster radius "rfms" in FEFF8) than to the whole-cluster size. This is the reason for the split appearing in the preedge peak of the spectrum calculated for the 45-atom cluster, not seen for smaller clusters and appearing as a shoulder

(22) Yokoyama, T.; Kobayashi, K.; Ohta, T.; Ugawa, A. *Phys. Rev. B* **1996**, *53*, 6111.
(23) Haskel, D. Ph.D. Thesis, University of Washington, 1997.
(24) Sakane, H.; Muñoz-Páez, A.; Díaz-Moreno, S.; Martínez, J. M.; Pappalardo, R. R.; Sánchez Marcos, E. *J. Am. Chem. Soc*. **1998**, *120*, 10397.
(25) Blixt, J.; Glaser, J.; Mink, J.; Persson, I.; Persson, P.; Sandström, M. *J. Am. Chem. Soc*. **1995**, *117*, 5089.
(26) Díaz-Moreno, S.; Martínez, J. M.; Muñoz-Páez, A.; Sakane, H.; Watanabe, I. *J. Phys. Chem. A* **1998**, *102*, 7435.

for the 78-atom cluster. The other features appearing in the XANES region are not affected significantly by this size. To investigate the effect of disorder, an additional calculation was made for the fully symmetric 9-atom structure, with averaged distances for Ni−C and Ni−N coordination shells. The result has been included in Figure 1b as well. It is seen that the disorder causes a shift in the main peaks of the spectrum but does not cause changes in the intensity ratio of the peaks or in the appearance of new features. As will be discussed later, the EXAFS region seems to be more sensitive to this type of structural disorder.

When discussing the effect of the cluster size, it is important to remember the remarkable similarity between the solid and the liquid samples. By examining Figure 1a, one would infer that the most significant scattering contributions are those occurring within essentially rigid 9-atom $[Ni(CN)_4]^{2-}$ units. Analyzing the spectroscopic features in terms of nuclear and electronic structures, we infer that, from the viewpoint of the central Ni atoms, the closer environment in aqueous solutions is very similar to the environment within the solid (i.e., four cyanide ligands strongly bonded) but locally even more ordered due to the relaxation of crystalline packing restrictions. In this sense, the local structure of the solution is more ordered than that of the solid, which is just the converse of the usual picture. Second-order perturbations due to specific and bulk solvent interactions can certainly affect the electronic and nuclear distributions of the anion complex, but it seems unlikely that they could cause changes similar to those produced by the environment present in the solid because, in this phase, counterions and other units of tetracyanonickelate replace the solvent molecules.

We were interested in the relative importance of MS paths in the XANES region. Using the FMS approach, it was possible to define a cutoff radius such that only MS paths with total path lengths smaller than $2r_c$ ("rclus2" in FEFF8) were considered. When only carbon atoms were taken into account ($r_c = 2.0$ Å), the XANES spectrum was rather different from that including carbon and nitrogen atoms. The two main peaks merged into one peaking at an intermediate value; however, the so-called preedge peak was retained showing a higher intensity. A similar behavior was reported by Bianconi et al. in a study of iron hexacyanide complexes.[12]

The special symmetry of the system, both within the molecular plane and within the packing in the crystal, produces polarization-sensitive spectra.[7−9] To check the capabilities of the FEFF code in this field, calculations of the spectra with *X*-, *Y*-, and *Z*-polarized light were performed for increasing cluster sizes. The corresponding plots are included in Figure 2 (for the sake of simplicity, *Y*-polarized spectra, which are very similar to *X*-polarized ones, are not included). *X* and *Y* axes are defined to be in the molecular plane matching molecular bonds. *X* axis corresponds to the shorter bond distances. The *Z* axis is defined by the chain of nickel atoms perpendicular to the molecular plane.

The *X*-polarized spectra, which are rather insensitive to cluster size, show the strongest modulation and are quite similar to the experimental spectra included in Figure 1a of ref 9. The *Z*-polarized spectrum calculated for a 9-atom cluster is very similar to that calculated for the 13-atom cluster of iron hexacyanide complexes,[12] but it fails to reproduce the sharp feature experimentally observed below the main rise ($b_1$). Although having weaker intensity, this feature is clearly visible for cluster sizes equal to or larger than 21 atoms. Higher cluster sizes (45 atoms) are required to adequately reproduce features $b_2$ and c after the edge.[7−9]

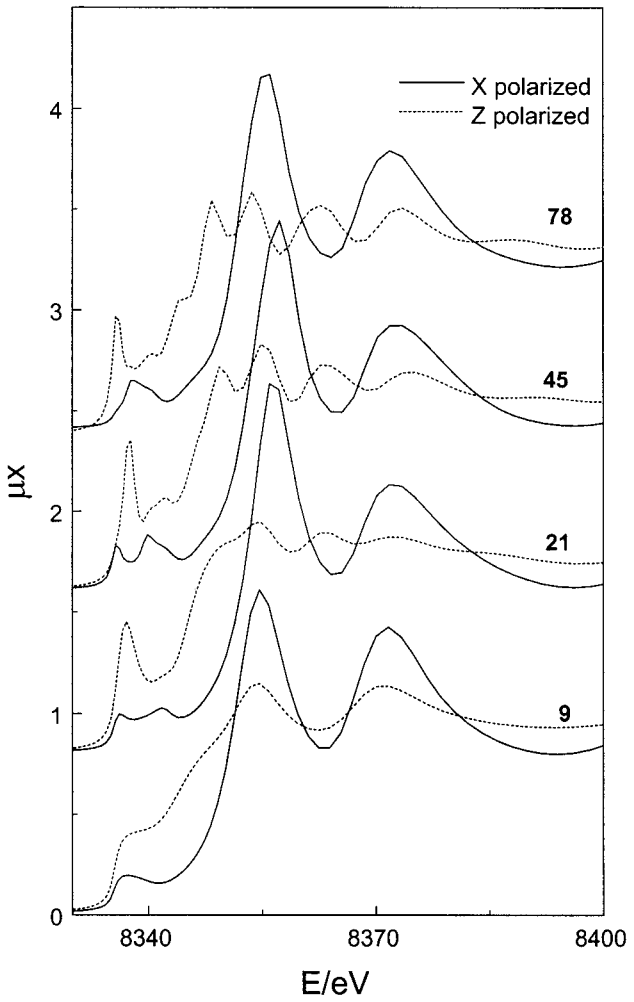


**Figure 2.** Computed XANES spectra of the 9-, 21-, 45-, and 78-atom clusters for *Z*-polarized light (dashed lines) and *X*-polarized light (solid lines). *X* and *Y* axes match Ni−C−N bonds; the *Z* axis matches Ni−Ni bonds perpendicular to the molecular plane.

Figure 3 includes comparative plots of the XANES spectrum calculated for the 78-atom cluster and of the Ni p-density of states, calculated on the basis of the fully relaxed core hole for the final state, which show that the XANES spectrum is proportional to a broadened p-DOS above the Fermi energy. As shown in this figure as well, the Fermi level, calculated by the SCF method, appears 10.4 eV below the initial estimate as the maximum in the first derivative of the main rise. It was found to lie in the middle of the band gap in the density of states diagram, a situation similar to that found in other insulator systems, such as BN and $PbTiO_3$.[18] The threshold thus found lies approximately 1 eV below the so-called "preedge peak" and well below the middle point of the main rise. In this context, a better definition of the preedge peak would be "a sharp feature within the edge structure".

**EXAFS Spectra.** Figure 4a shows the magnitudes of the phase-corrected Fourier transforms ($k^3$; $\Delta k = 3.1-13$ Å$^{-1}$) of the raw EXAFS spectra of the solid and solution systems. (Raw data have been included as Supporting Information in Figure S1a.) Two peaks of similar intensities, centered at approximately 1.8 and 3.0 Å, appear in both Fourier transforms. On the basis of the most probable structure of the complex, these peaks can be attributed unambiguously to the dominant Ni−C and Ni−N contributions. The amplitude of the second peak in the FT is

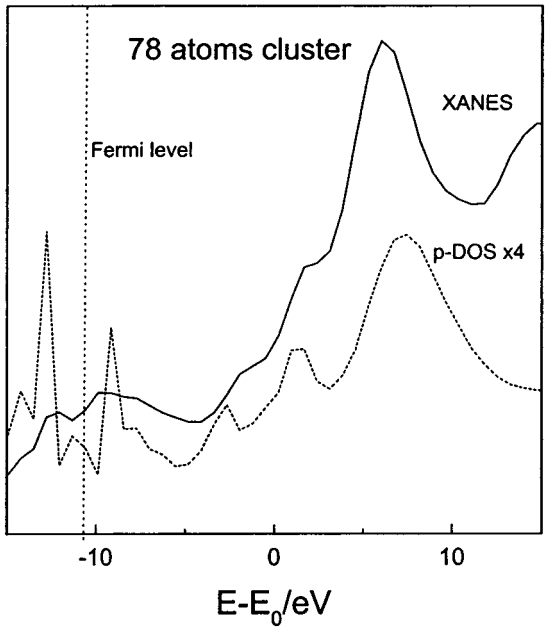


**Figure 3.** Computed XANES spectrum for the 78-atom cluster (solid line) and a Ni p-density of states diagram (dashed line).

strikingly high. Indeed, if one takes into account *only* single-scattering (SS) contributions, the amplitude of this contribution should be quite small (see Figure 4c). Since this is not the case, multiple-scattering (MS) contributions must play an important role in this system. Another unusual feature in this plot is the higher amplitude of the signal corresponding to the solution compared to that of the solid. Due to the typically higher dynamic disorder of the liquid state, the effect on peak amplitudes observed in most cases is just the opposite.[26]

The geometry around the Ni sites, as published from XRD data,[4a] was used for the calculations of the MS path contributions employing the FEFF8 code, yielding 16 scattering paths. This number was reduced to 8 when a calculation was performed using the geometry of the symmetric square planar complex obtained by averaging the values of the crystalline anhydrous potassium salt, i.e., Ni−C bond distance at 1.870 Å and Ni−N at 2.994 Å. Since there was no significant difference in the results or in the quality of the fit when the averaged or the split structure was used, as already observed by other authors for inclusion compounds containing the $[Ni(CN)_4]^{2-}$ units,[10] the averaged structure was employed in all subsequent calculations, using the eight scattering paths shown in Scheme 1. Paths 1 and 2 correspond to SS contributions of the first and second coordination shells, whereas paths 3 and 4, which have remarkably high amplitudes, correspond to three- and four-legged forward-focused linear paths. This focusing effect has been observed in many other systems having aligned atoms.[26−31] In contrast, paths 5 and 8 have smaller amplitudes.

The Debye−Waller factors of the MS paths were obtained, as described above, with the aid of the independent-vibration model.[22] In this way, Debye−Waller factors, $\sigma^2$, for paths 3−8

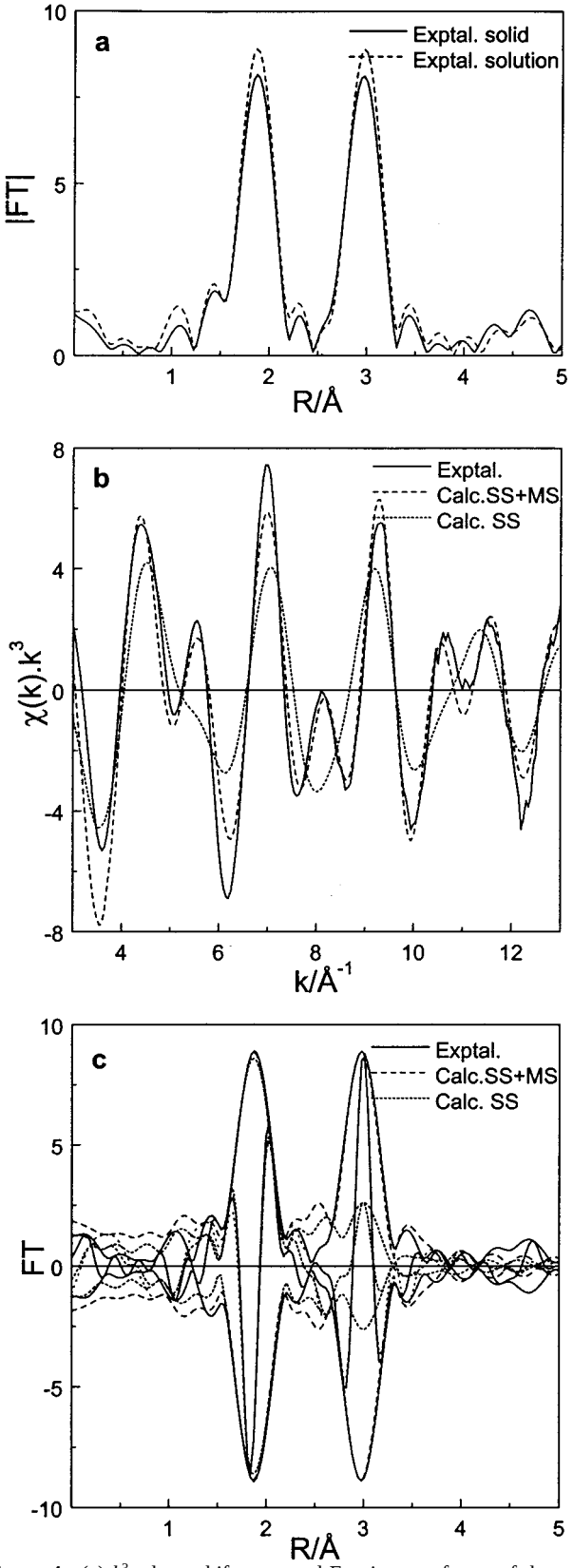


**Figure 4.** (a) $k^3$, phase-shift-corrected Fourier transforms of the raw EXAFS data for $K_2[Ni(CN)_4]$ in the solid state (solid line) and in a 0.1 *m* aqueous solution (dashed line). (b) Raw EXAFS data (solid line), data best-fit with parameters included in Table 1 (dashed line), and data best-fit with single-scattering contributions only (dotted line) for the dissolved species $[Ni(CN)_4]^{2-}$. (c) Phase-shift-corrected Fourier transforms of the spectra included in Figure 4b.

were defined as functions of the Debye−Waller factors for paths 1 and 2, the only exception being the case of triangular path 5,

(27) Kuzmin, A.; Purans, J.; Parent, Ph. *Physica B* **1995**, *208*−*209*, 45.
(28) O'Day, P. A.; Rehr, J. J.; Zabinsky, S. I.; Brown, G. E. *J. Am. Chem. Soc.* **1994**, *116*, 2938.
(29) Scott, M. J.; Zhang, H. H.; Lee, S. C.; Hedman, B.; Hodgson, K. O.; Holm, R. H. *J. Am. Chem. Soc.* **1995**, *117*, 568.
(30) Van der Gaauw, A.; Wilkin, O. W.; Young, N. A. *J. Chem. Soc., Dalton Trans.* **1999**, 2405.
(31) Ressler, T.; Brock, S. L.; Wong, J.; Suib, S. L. *J. Phys. Chem. B* **1999**, *103*, 6407.

**Scheme 1.** More Intense Scattering Paths Indicating the Values of Relative Amplitudes for Zero Debye−Waller Factors

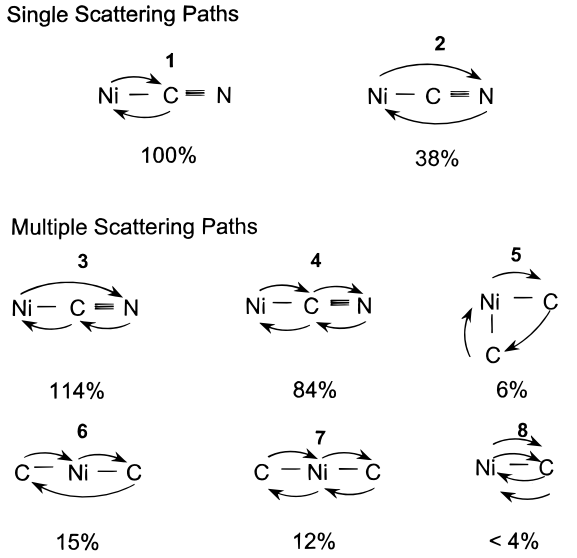


which has a different and higher value of $\sigma^2$. The definitions for the mean square displacements of the paths are as follows:

$$\sigma^2(\text{Ni}-\text{C})_1 = \sigma^2{}_1 \qquad \sigma^2(\text{Ni}-\text{N})_2 = \sigma^2{}_2$$

$$\sigma^2(\text{Ni}-\text{C}-\text{C})_5 = \sigma^2{}_5$$

$$\sigma^2(\text{Ni}-\text{N}-\text{C})_3 = \sigma^2(\text{Ni}-\text{C}-\text{N}-\text{C})_4 = \sigma^2{}_2 \qquad (1)$$

$$\sigma^2(\text{Ni}-\text{C}-\text{C})_6 = \sigma^2(\text{Ni}-\text{C}-\text{Ni}-\text{C})_7 \cong 2\sigma^2{}_1 \qquad (2)$$

$$\sigma^2(\text{Ni}-\text{C}-\text{Ni}-\text{C})_8 = 4\sigma^2{}_1 \qquad (3)$$

The only requirement to be fulfilled in eq 1, is that the Ni, C, and N atoms be aligned. Equation 2 is applicable in the limit of medium to high temperatures, and eq 3 is always fulfilled, since it only takes into account the definition of $\sigma^2$.[23]

Alternatively, DW factors were obtained from the Debye-correlated model, by fitting the Debye temperature, which turned out to be 1621 K. This strikingly high value could be related to the C−N triple bonds. The values of DW factors obtained for SS and MS paths using this model were very similar to those obtained using the independent-vibration model.

In a preliminary analysis, the obtained value for the Debye−Waller factor of triangular path **5**, $\sigma^2{}_5$, was very high, which rendered the amplitude of its EXAFS contribution very small, as observed in other systems.[26−30] Although the amplitudes of paths **6**−**8** in principle were not negligible and, in fact, these types of paths are relevant in symmetric complexes showing only one coordination shell, such as hexahydrates[24] and tetrahalides,[30] in the present system these amplitudes were irrelevant when compared to those of paths **1**−**4**. Thus, during the final fitting procedure, only paths **1**−**4** were considered. The amplitude reduction factor $S_0{}^2$ was set equal to 1 for both systems. In this way, only *five free parameters* need to be considered: the inner potential correction $\Delta E_0$, the Debye−Waller factors for paths **1** and **2**, $\sigma^2{}_1$ and $\sigma^2{}_2$, and the respective interatomic distances for the Ni−C and Ni−N contributions.

The parameters obtained for the best fits of the solid and liquid systems are given in Table 1. As seen there, good fits are obtained with closely similar sets of parameters, the main difference being the slightly higher values of $\sigma^2$ obtained for the solid system. The values obtained for the Ni−N distances are slightly larger than those of the initial structure (3.03 vs 2.99 Å), but no significant changes (less than 0.01 Å) in the Ni−C distances compared to the starting values were observed. These values are very similar to those obtained for related systems,[10] in which 1.86 Å was obtained for the Ni−C bond distances and 3.01 Å for the Ni−N distances.

**Table 1.** Best-Fit Parameters Obtained in the Analysis of the EXAFS Spectra of Solid $K_2[Ni(CN)_4]$ and the Dissolved System (0.1 *m* Aqueous Solution)[a]

| | solution | solid |
|---|---|---|
| $\Delta E_0$, eV | 7.9 ± 1.5 | 5.9 ± 1.2 |
| $\sigma_1{}^2$(Ni−C), Å$^2$ | 0.0040 ± 0.001 | 0.0045 ± 0.0007 |
| $\sigma_2{}^2$(Ni−N), Å$^2$ | 0.0055 ± 0.001 | 0.0057 ± 0.0006 |
| *R*(Ni−C), Å | 1.862 ± 0.010 | 1.861 ± 0.008 |
| *R*(Ni−N), Å | 3.03 ± 0.011 | 3.03± 0.011 |
| *R* factor | 0.08 | 0.11 |
| $\chi^2$ | 3825 | 5063 |
| $\chi_\nu{}^2$ | 297 | 300 |

[a] $\Delta R = 1.0-3.5$ Å; $\Delta k = 3.0-13.0$ Å$^{-1}$; $k^3$.

**Table 2.** Structural Parameters for Systems Containing $[Ni(CN)_4]^{2-}$ Units (from Ref 4)

| compound | $\Delta R$(Ni−C), Å | $\Delta R$(Ni−N), Å | *R*(Ni−Ni), Å | rotation, deg |
|---|---|---|---|---|
| $K_2[Ni(CN)_4]$ | 0.06 | 0.09 | 4.3 | 0 |
| $CsK[Ni(CN)_4]$ | 0.04 | 0.05 | 4.3 | 35 |
| $Ba[Ni(CN)_4]\cdot 4H_2O$ | 0.002 | 0.02 | 3.36 | 45 |
| $Sr[Ni(CN)_4]$ | 0.0 | 0.0 | 8.31 | |
| $(C_7H_8N)_2[Ni(CN)_4]$ | 0.0 | 0.0 | 8.3 | not chain |
| $(C_6H_7N)_2[Ni(CN)_4]$ | 0.02 | 0.0 | | not chain |
| $(C_7H_9N)_2[Ni(CN)_4]\cdot 3H_2O$ | 0.04 | 0.03 | | not chain |
| aqueous solution | 0.0 | 0.0 | | |

Comparative plots of experimental EXAFS spectra for the dissolved species and of the spectra calculated with and without multiple-scattering contributions are shown in Figure 4b, while the corresponding magnitude and imaginary part of the phase-corrected Fourier transform appear in Figure 4c. Fairly good reproductions of the first peak of the Fourier transform can be achieved with and without MS contributions. In contrast, the second peak cannot be reproduced unless multiple-scattering contributions are taken into account. The need for the inclusion of multiple-scattering contributions is clear through the entire *k* range (see Figure 4b).

Comparison of the magnitudes for the FT's of paths **1**−**4** calculated for the liquid system indicates that the main contributions to the second peak in the experimental FT arise from focusing MS paths. Even more, taking into account the amplitude of each of these paths, the intensity of the second peak in the experimental FT might be expected to be even higher. But the EXAFS functions calculated for path **2** (SS Ni−N) and for path **4** (three-legged MS Ni−N) are opposite in phase and thus partially cancel each other. (See Figure S1b,c in the Supporting Information.)

Although small differences (within the limits of accuracy) have been found between the values of Debye−Waller factors for the solid and dissolved systems, they are large enough to make the amplitude of the FT for the solid smaller than that of the FT for the dissolved species. This can be related to the above-mentioned split in the structures of $[Ni(CN)_4]^{2-}$ units, which depend on the degree of hydration, the countercation, and the type of configuration adopted, i.e., eclipsed or staggered, which in turn determines the Ni−Ni distances (see Table 2). For the anhydrous potassium salt, the split in distances within the first and second coordination shells, $\Delta R$(Ni−C) = 0.06 Å and $\Delta R$(Ni−N) = 0.09 Å, introduces a high "static" disorder,

which is responsible for the observed decrease in amplitude in its EXAFS spectrum. In contrast, for the solution system, in which there are no packing restrictions, the most stable species seems to be the perfectly symmetric square planar complex. When the solid-state spectrum is fit with *one* shell for Ni−C and *one* shell for Ni−N contributions, the higher DW factor observed accounts for this "static" disorder, overcoming the higher dynamic disorder expected in the liquid system.

## Concluding Remarks

Although a reasonable reproduction of the XANES region of solid-state spectra has been obtained for a cluster formed by the basic $[Ni(CN)_4]^{2-}$ unit (9 atoms) and a significant number of shells around it (ca.70 atoms or more), the most striking feature of this region of the absorption spectra is the close similarity between the solid and solution systems, where the only well-defined entities are $[Ni(CN)_4]^{2-}$ units. This similarity brings into question the presumed sensitivity of XANES to long-range order and the usual approach in XANES investigations, in which a monotonic improvement in the reproduction of XANES spectra is associated with increasing cluster size. This leads one to wonder whether the standard approach for the study of XANES spectra, based on uniform convergence with cluster size,[32−34] is indeed the correct one or rather whether convergence may be slowed by significant fluctuations. To gain deeper insight into this open question, two lines of research should be undertaken and probably combined. The first one involves the inspection and refinement of the methodological approach used to compute the XANES spectra. The second involves statistical simulations to obtain a reasonable description of the solvation environment of these basic units[35] and then to compute the XANES spectrum with this more complete structure of the dissolved species.

A simple procedure has been proposed to handle the resolution of an EXAFS spectrum in which the major contributions arise from multiple-scattering terms: the amplitudes of the paths initially calculated with FEFF are estimated by determining the mean square displacement for MS with the aid of a simple model, and those irrelevant can be discarded. In this way, the total number of significant paths of this system, a paradigm of MS contributions, is reduced to 2 SS + 2 MS. The same values for Ni−C (1.86 Å) and Ni−N (3.03 Å) coordination distances were obtained for the solid-state and solution complexes. The split in Ni−C and Ni−N distances, similar to that observed in other solid systems including $[Ni(CN)_4]^{2-}$ units, although not resolved in the EXAFS spectrum, produces a static disorder that yields higher DW factors for the solid-state complex.

**Acknowledgment.** We thank A. Ankudinov for suggestions and advice regarding the FEFF8 code and I. Watanabe, H. Sakane, T. Miyanaga, and J. M. Martinez for their assistance during the recording of the EXAFS spectra. Thanks are also expressed to the Photon Factory of the Institute of Material Structure Science (Project No. 95-G215) at KEK, Tsukuba, Japan, for beamtime allocation and to the Spanish DGICYT (Project No. PB98-1153) and the U.S. DOE (Grant DE-FG03-97ER45623) for financial support.

**Supporting Information Available:** Input and output files for FEFF and FEEFIT program codes (Tables IS−IVS), raw EXAFS data for $K_2[Ni(CN)_4]$ in the solid state and in 0.1 *m* aqueous solution (Figure S1a), magnitudes of the phase-shift-corrected Fourier transforms of the EXAFS contributions calculated for paths 1−4 with parameters included in Table 1 for the dissolved species (Figure S1b), and EXAFS signals calculated for paths 2 and 4 with the parameters of the liquid system (Figure S1c). This material is available free of charge via the Internet at http://pubs.acs.org.

IC000274N

(32) Farges, F.; Brown, G. E.; Rehr, J. J. *Phys. Rev. B* **1997**, *56*, 1809.
(33) Ruiz-López, M. F.; Muñoz-Páez, A. *J. Phys. Condens. Matter* **1991**, *2*, 8981.
(34) Wu, Z. Y.; Ouvrad, G.; Natoli, C. R. *J. Phys. IV* **1997**, *7*, C2-199.
(35) Campbell, L.; Rehr, J. J.; Schenter, G. K.; McCarthy, M. I.; Dixon, D. *J. Synchrotron Rad.* **1999**, *6*, 310.